

## ORIGINAL COMMUNICATION

# The Fasciocytes: A New Cell Devoted to Fascial Gliding Regulation

CARLA STECCO <sup>1,\*</sup> CATERINA FEDE,<sup>1</sup> VERONICA MACCHI,<sup>1</sup> ANDREA PORZIONATO,<sup>1</sup> LUCIA PETRELLI,<sup>1</sup> CARLO BIZ,<sup>2</sup> ROBERT STERN,<sup>3</sup> AND RAFFAELE DE CARO<sup>1</sup>

<sup>1</sup>Department of Neuroscience, University of Padova, via Gabelli 65, Padova, 35121, Italy

<sup>2</sup>Department of Surgery, Oncology and Gastroenterology DiSCOG, Orthopedic Clinic, University of Padova, via Giustiniani 2, Padova, 35121, Italy

<sup>3</sup>Division of Basic Biomedical Sciences, Touro College of Osteopathic Medicine, 230 West-125th Street, New York, New York, 10027

Hyaluronan occurs between deep fascia and muscle, facilitating gliding between these two structures, and also within the loose connective tissue of the fascia, guaranteeing the smooth sliding of adjacent fibrous fascial layers. It also promotes the functions of the deep fascia. In this study a new class of cells in fasciae is identified, which we have termed fasciocytes, devoted to producing the hyaluronan-rich extracellular matrix. Synthesis of the hyaluronan-rich matrix by these new cells was demonstrated by Alcian Blue staining, anti-HABP (hyaluronic acid binding protein) immunohistochemistry, and transmission electron microscopy. Expression of HAS2 (hyaluronan synthase 2) mRNA by these cells was detected and quantified using real time RT-PCR. This new cell type has some features similar to fibroblasts: they are positive for the fibroblast marker vimentin and negative for CD68, a marker for the monocyte-macrophage lineage. However, they have morphological features distinct from classical fibroblasts and they express the marker for chondroid metaplasia, S-100A4. The authors suggest that these cells represent a new cell type devoted to the production of hyaluronan. Since hyaluronan is essential for fascial gliding, regulation of these cells could affect the functions of fasciae so they could be implicated in myofascial pain. Clin. Anat. 00:000–000, 2018. © 2018 Wiley Periodicals, Inc.

**Key words:** fasciocytes; hyaluronan; extracellular matrix; fascia

## INTRODUCTION

The deep fascia is a multilayered structure formed by two to three layers of densely-packed collagen fibers with a few elastic fibers, separated by layers of loose connective tissue (Benetazzo et al., 2011), rich in hyaluronan (HA). It is widely recognized that fasciae have an active role in tissue maintenance and repair. They are abundantly innervated and rich in proprioceptors, vascular channels, and lymphatic channels (Stecco et al., 2007; Bhattacharya et al., 2011). Fascia has a multitude of functions including force transmission, movement, stability, proprioceptive communication throughout the body, and in promoting sliding and reducing the friction associated with motion (Kumka and Bonar, 2012). To ensure proper function it is important that the loose connective tissue within

fascial sublayers has the correct status, including orientation and organization.

Thickening and a densification of the loose connective tissue and its extracellular matrix (ECM) correspond to the reduction or loss of fascial sliding ability (Langevin et al., 2011; Chaitow, 2014). If the connective tissue is lost or its density is altered, the behavior of the deep fascia and underlying muscle becomes compromised. This could be the source of myofascial

\*Correspondence to: Carla Stecco, Section of Anatomy, Department of Neuroscience, University of Padova, via A. Gabelli 65, 35121 Padova, Italy. E-mail: carla.stecco@unipd.it

Received 21 February 2018; Accepted 13 March 2018

Published online in Wiley Online Library (wileyonlinelibrary.com). DOI: 10.1002/ca.23072

pain in many cases. One key element affecting fascia density seems to be HA (Stecco et al., 2014).

HA is synthesized within the plasma membranes of most cell types by membrane-bound synthases. The chains are extruded into the extracellular space through pore-like structures (Jiang et al., 2007). The resulting HA serves a range of functions including space filling, lubrication of joints, water homeostasis, and provision of a matrix that facilitates cell migration (Fraser et al., 1997; Cowman et al., 2015). In recent years, it has also been demonstrated that HA provides a substrate for the smooth gliding of different motor units between and within muscle (McCombe et al., 2001).

Previous work from this laboratory revealed fibroblast-like cells on the inferior surface of the deep fascia that stained prominently with Alcian Blue. We suggested that these cells were related to other fibroblast-like cells in the vertebrate body but were specialized for HA synthesis and secretion (Stecco et al., 2011), similar to the synoviocytes on the inner surfaces of joint capsules (Chang et al., 2010) that synthesize the HA-rich synovial fluid, and the hyalocytes in the eye that elaborate the HA-rich humors of the anterior and posterior chambers (Sakamoto and Ishibashi, 2011). We suggested that they represent a previously-unidentified class of cells that we called "fasciocytes." Fasciocytes have not yet been analyzed morphologically and immunohistochemically; this is the purpose of the current study. Here, we characterize this new cell type, demonstrating that they differ in morphological features and immunoreactivity from classical fascial fibroblasts. Showing that they are specialized for the biosynthesis of a HA-rich matrix helps to elucidate the role of HA in conferring viscoelasticity of fascial tissue under healthy conditions, and in a myriad of pathophysiological conditions that include myofascial pain, disuse atrophy, hypertrophy, and the fascia associated with muscle scarring, contractures, and fibrosis.

## MATERIALS AND METHODS

### Sample Collection

This study was approved by our Institutional Ethical Review Board (approval no. 3722/AO/16). The institute's ethical regulations for research conducted on human tissues were followed. Written informed consent was obtained from each donor.

Samples of fascia lata (1 cm × 1 cm) were collected from 12 volunteer patients, five males and seven females, average age 76 ± 11 years. They were all undergoing elective surgery at the Orthopedic Clinic of Padova University (total hip prosthesis, anterolateral approach). The samples were transported to the laboratory in phosphate-buffered saline (PBS) within a few hours of collection.

Each sample was divided into three sections: one was frozen or maintained in PBS and used fresh for real-time PCR; the second was formalin-fixed for histology; and the third was fixed in 2.5% glutaraldehyde for transmission electron microscopy.

### Morphological Analysis and Differential Staining of Glycosaminoglycans

Each of the formalin-fixed human fascia specimens (0.5 cm × 0.5 cm) was dehydrated in graded ethanol, embedded in paraffin and cut into 6 μm-thick sections. The following histochemical stains were applied to each dewaxed section: Hematoxylin and eosin (H&E), and 0.05% Alcian Blue pH 5.8, which stains acidic polysaccharides such as glycosaminoglycans (GAGs). In parallel, dewaxed sections were pretreated overnight at 37°C with 2 mg/mL hyaluronidase (from bovine testes, Sigma Aldrich) and then subjected to the protocols described. As positive controls, human umbilical cords from volunteer women were used (data not shown).

The critical electrolyte concentration (CEC) principle was applied for the Alcian Blue staining procedure: different concentrations of MgCl<sub>2</sub> (0.025 M to 2 M) cause differences in staining because the cations of the salt compete with those of the dye for the polyanionic sites in the tissue (Scott and Dorling, 1965). Dewaxed sections were incubated for 1 hr in sodium acetate buffer, pH 5.8, with 0.05 M or 2 M MgCl<sub>2</sub>, and then stained with 0.05% Alcian Blue with the same concentrations of MgCl<sub>2</sub> as in the buffer solution for a total of 4 hr. The tissues were then washed in 0.01 N HCl for 10 min and in distilled water. The nuclei in tissue sections were counterstained with ready-to-use hematoxylin (Dako). Dehydrated samples were mounted with a coverslip using Eukitt (Agar Scientific).

Images were obtained using a Leica DMR microscope (Leica Microsystems, Wetzlar, Germany; objectives 20× and 40×, Leica) and analyzed using Image J software.

### Immunohistochemistry to Detect HABP (Hyaluronic Acid Binding Protein)

All the formalin-fixed specimens (0.5 cm × 0.5 cm) were dehydrated in graded ethanol, embedded in paraffin and cut into 6 μm-thick sections as described above. In parallel, dewaxed sections were pretreated overnight at 37°C with 2 mg/mL hyaluronidase. Afterwards, all samples were subjected to the protocols described below.

Dewaxed sections were treated with avidin and biotin solutions (20 min each at RT) to block endogenous avidin biotin activity. Endogenous peroxidase was blocked with 0.5% H<sub>2</sub>O<sub>2</sub> in PBS for 5 min at RT, and then the specimens were washed with PBS, incubated in 0.1% BSA for 1 hr at RT, treated with biotinylated 2 μg/mL HABP (Amsbio), diluted with the same pre-incubation buffer, and incubated overnight at 4°C. After repeated PBS washing, the samples were incubated with the secondary antibody HRP-conjugated Streptavidin (1:250) for 30 min (Jackson ImmunoResearch) and washed in PBS. The reaction was then developed with 3,3'-diaminobenzidine (Liquid DAB + substrate Chromogen System kit, Dako Corp, Carpinteria, CA) and the reaction was terminated with distilled water.

For negative controls, similarly-treated sections were used omitting the primary antibody. This confirmed the specificity of the immunostaining reaction. As positive

**TABLE 1. Sense and Antisense Sequences used as RT-PCR Primers**

Sequence name	Acc. number	BP	Primers
RPS18 F142	NM_022551	111	5'-ATT AAG GGT GTG GGC CGA AG -3'
RPS18 R252			5'-GGT GAT CAC ACG TTC CAC CT -3'
RPLP0 F824	NM_053275	95	5'- GCA GCA TCT ACA ACC CTG AA-3'
RPLP0 R918			5'-CAG ACA GAC ACT GCC AAC AT-3'
HAS2 F1233	NM_005328	253	5'-ATC CCA TGG TTG GAG GTG TT-3'
HAS2 R1485			5'-TGC CTG TCA TCA CCA AAG CT -3'

controls we used human umbilical cords from female volunteers. The nuclei in tissue sections were counterstained with ready-to-use hematoxylin (Dako Corp, Carpinteria, CA).

Images were recorded using a Leica DMR microscope (Leica Microsystems, Wetzlar, Germany).

### TEM (Transmission Electron Microscopy) Analysis

Four specimens of human fascia lata (dimensions: 0.5 cm × 0.5 cm) were fixed in 0.1 M phosphate-buffered 2.5% glutaraldehyde (Serva Electrophoresis, Heidelberg, Germany), post-fixed in 1% osmium tetroxide (OsO<sub>4</sub>) (Agar Scientific Elektron Technology, Stansted, UK) in 0.1 M phosphate buffer, dehydrated in a graded ethanol series, and embedded in Epoxy Embedding Medium Kit (45349, Sigma-Aldrich, St. Gallen, Switzerland). Semithin (0.5 μm) and ultrathin (60 nm) sections were cut with an RMC Power-Tome ultramicrotome (Boeckeler Instruments, AZ). Semithin sections were stained with 1% Toluidine blue; ultrathin sections were collected on 300-mesh copper grids and counterstained with 1% uranyl acetate and then Sato's lead. The specimens were examined with a Hitachi H-300 Transmission Electron Microscope.

### Characterization of Fasciocytes

The following immunohistochemical stains were applied to each of the formalin-fixed human fascia lata specimens: anti-vimentin (monoclonal mouse antibody, Invitrogen; dilution 1:250), anti-CD68 (monoclonal mouse antibody, DakoCytomation; dilution 1:100), and anti-S-100A4 (polyclonal rabbit antibody, Abcam; dilution 1:100). The marker S-100A4 was selected to demonstrate that fasciocytes are cells undergoing chondroid metaplasia.

Indeed, Klein et al. (1999) demonstrated that in the extensor retinaculum of the wrist and ankle there are scattered HA-secreting cells, positive for S-100 protein. S-100A4 belongs to the family of calcium-binding S-100 proteins that are not only specific for neuronal and glial elements (Castagna et al., 2003) but also occur in cells of different origins and functions (Mohr et al., 1985). S-100 is a multifunctional protein involved in matrix remodeling (Yammani et al., 2009) and in regulating several cellular processes such as motility, growth and differentiation, structural organization of membranes, protection against oxidative damage, protein phosphorylation, and secretion (Sedaghat and Notopoulos, 2008). Recently, S-100A4 was used as a marker to follow cancer progression (Fei et al.,

2017), as a mesenchymal marker (Seccia et al., 2016), and as a marker of chondroid metaplasia (Klein et al., 1999; Taşdemir et al., 2014).

Briefly, dewaxed sections were incubated with 0.1% trypsin in 0.05%-calcium chloride, pH 7.8, for 15 min at 37°C to unmask the antigens (for the S-100A4 stain), or maintained at 96°C for 15 min in sodium citrate, pH 6.0, for heat-induced antigen retrieval (for vimentin and CD68). Endogenous peroxidases were blocked with 0.5% H<sub>2</sub>O<sub>2</sub> in distilled water for 5 min at room temperature and then washed. Specimens were then incubated in 1% BSA-0.2% Triton-X for 1 hr at RT, and then incubated overnight at 4°C with the primary antibody diluted in the same pre-incubation buffer. After repeated PBS washing, samples were incubated with the secondary antibody Advance HRP Detection System (Dako Corp., Carpinteria, CA), ready-to-use, for mouse and rabbit, and washed in PBS. The reaction was then developed with 3,3'-diaminobenzidine (Liquid DAB + substrate Chromogen System kit Dako Corp, Carpinteria, CA) and stopped with distilled water. Sections incubated without primary antibodies showed no immunoreactivity, confirming the specificity of the immunostaining.

The images were acquired using a Leica DMR microscope (Leica Microsystems, Wetzlar, Germany) and S-100A4 positive cells were counted manually (total number of cells counted >3,500).

### Real-Time PCR

The biosynthesis of HA is dictated by three members of the hyaluronan synthase family (HAS1, HAS2, and HAS3), of which HAS2 is the most important and most highly expressed (Camenisch et al., 2000). We therefore detected and studied the expression of HAS2 mRNA by real time RT-PCR.

Briefly, four tissue specimens (1 cm × 0.5 cm) were homogenized in RNA lysis buffer, and total RNA was extracted using the SV Total RNA Isolation System (Promega Corporation, Madison, WI) and purified. DNase was used during RNA extraction to remove genomic DNA contamination. The total RNA was then reverse-transcribed to cDNA using the iScript cDNA Synthesis Kit (BioRad Laboratories, Milan, Italy). RT-PCR was performed in an I-Cycler iQ detection system (BioRad), using the primers reported in Table 1, and a 30 ng starting amount of cDNA denaturation step at 95°C for 3 min, 45 cycles of three amplification steps (15s 95°C / 15s 60°C for RPS18 and RPLP0, 15s 64°C for HAS2 /15s 72°C), and a melting curve (60–90°C with a heating rate of 0.5°C/10 s).

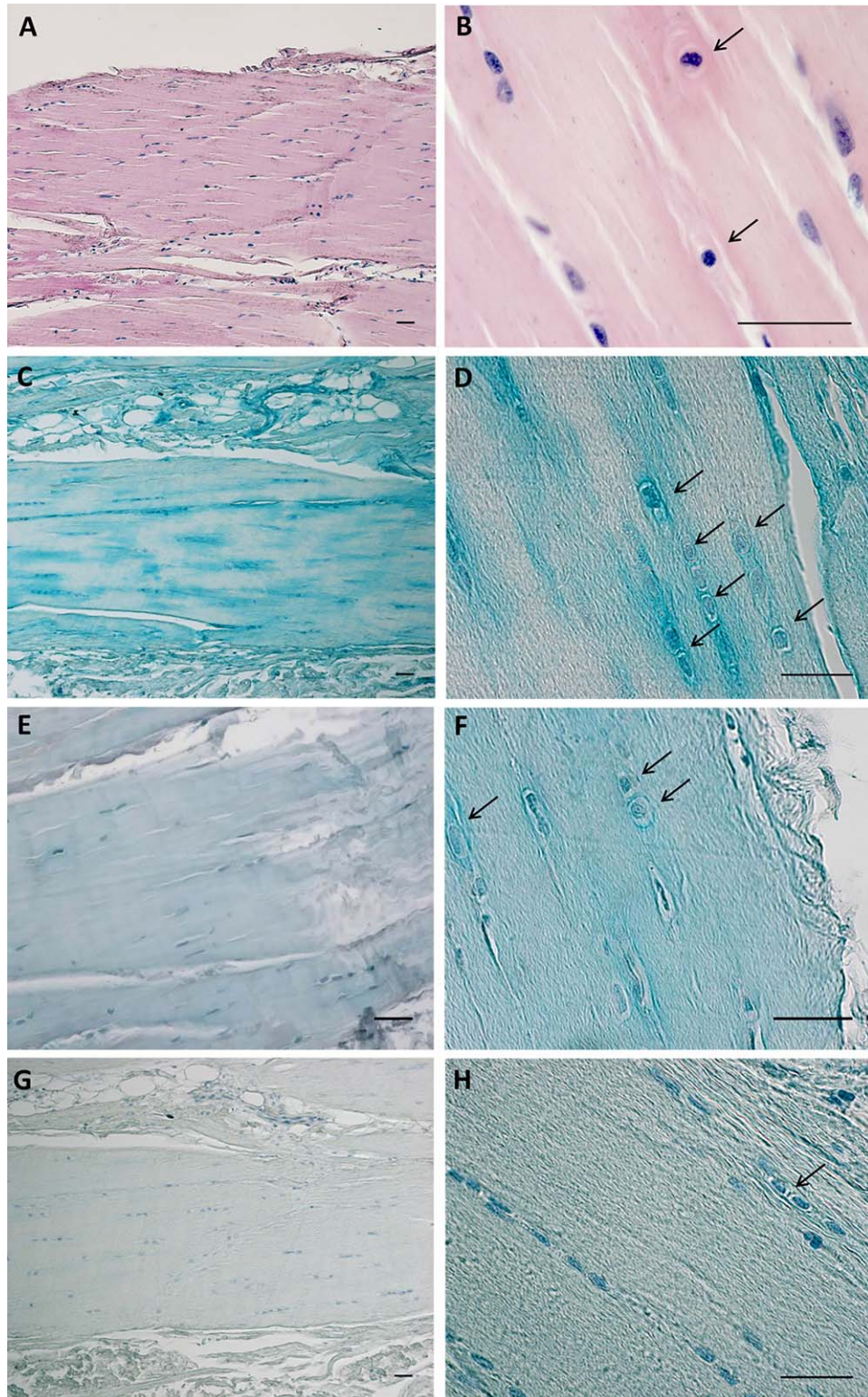


**Fig. 1.** Hematoxylin & Eosin staining (A,B) and Alcian blue staining of paraffin sections of human fascia lata. C,D are stained with 0.05% Alcian Blue/MgCl<sub>2</sub> 0.05 M in sodium acetate buffer for GAGs; E,F are stained with 0.05% Alcian Blue/2 M MgCl<sub>2</sub> specifically for HA and chondroitin sulfate;

and G,H are incubated with hyaluronidase (overnight at 37°C) and then stained with 0.05% Alcian Blue/0.05 M MgCl<sub>2</sub>. Arrows indicate prominent rounded nuclei with abundant extracellular matrix. Scale bars: (A-H), 50 μm. [Color figure can be viewed at [wileyonlinelibrary.com](http://wileyonlinelibrary.com)]

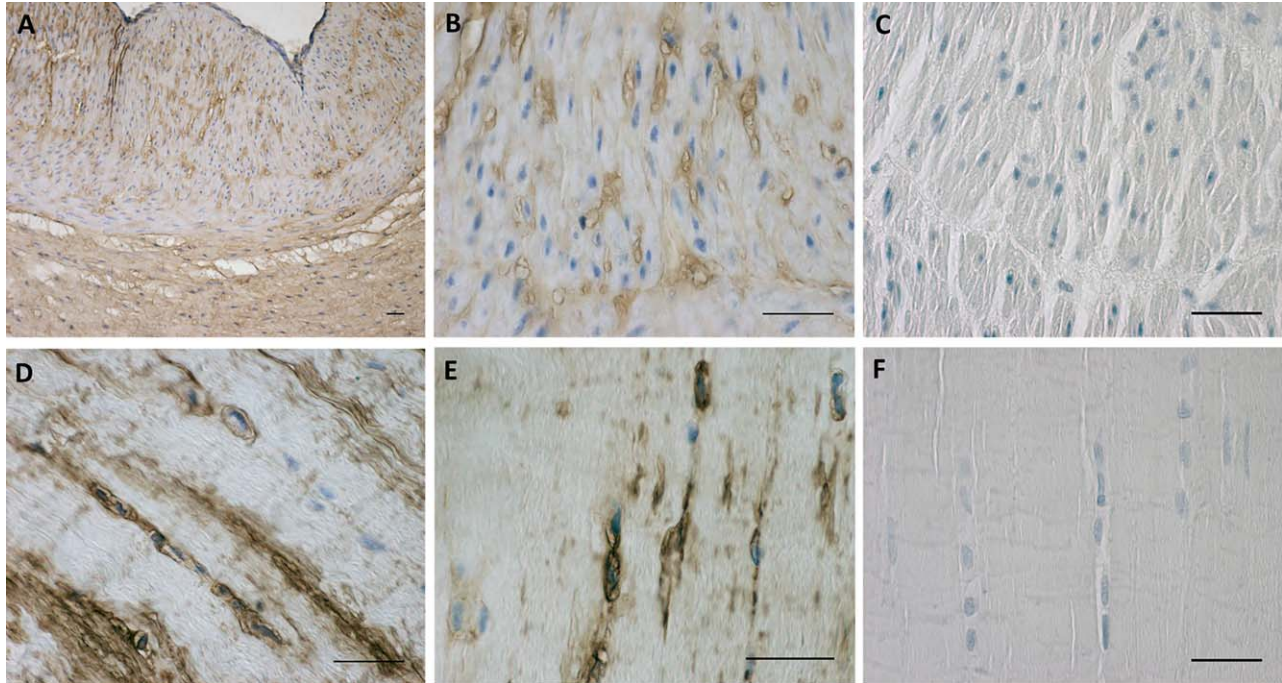


**Fig. 2.** HABP expression in human umbilical cord (A,B,C) and in human fascia lata (D,E,F). C and F are incubated with hyaluronidase (overnight at 37°C) before the immunostaining. Scale bars: (A–F), 50  $\mu\text{m}$ . [Color figure can be viewed at [wileyonlinelibrary.com](http://wileyonlinelibrary.com)]

During the exponential phase, the fluorescence signal threshold was calculated and the number of PCR cycles required to reach the threshold (cycle threshold, Ct) was determined. Ct values decreased linearly with increasing quantity of input target. All samples were amplified in duplicate and expressions of RPS18 (Ribosomal Protein S18) and RPLP0 (ribosomal protein lateral stalk subunit P0) were used as a reference. The specificity of the

amplification was tested at the end of each run by melting curve analysis, using I-Cycler software 3.0.

## RESULTS

We found some rounded cells in all the fascial samples, already evident using H&E staining: they are

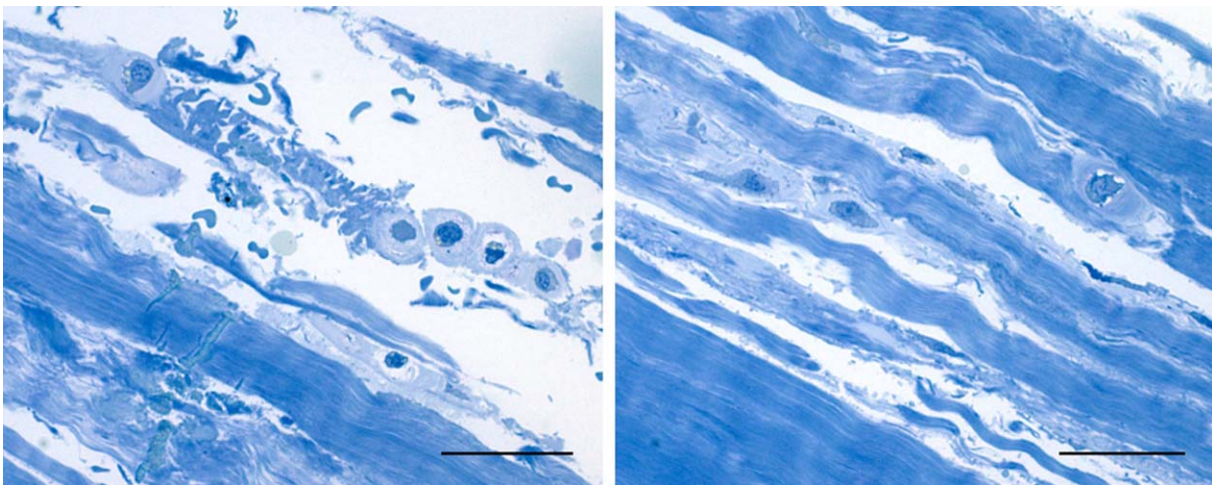


**Fig. 3.** Semithin sections stained with 1% Toluidine blue. Left image: fasciocytes in the external loose connective tissue; right image: fasciocytes in the loose connective tissue between the fibrous fascial layers. Scale bars: 100  $\mu\text{m}$ . [Color figure can be viewed at [wileyonlinelibrary.com](http://wileyonlinelibrary.com)]

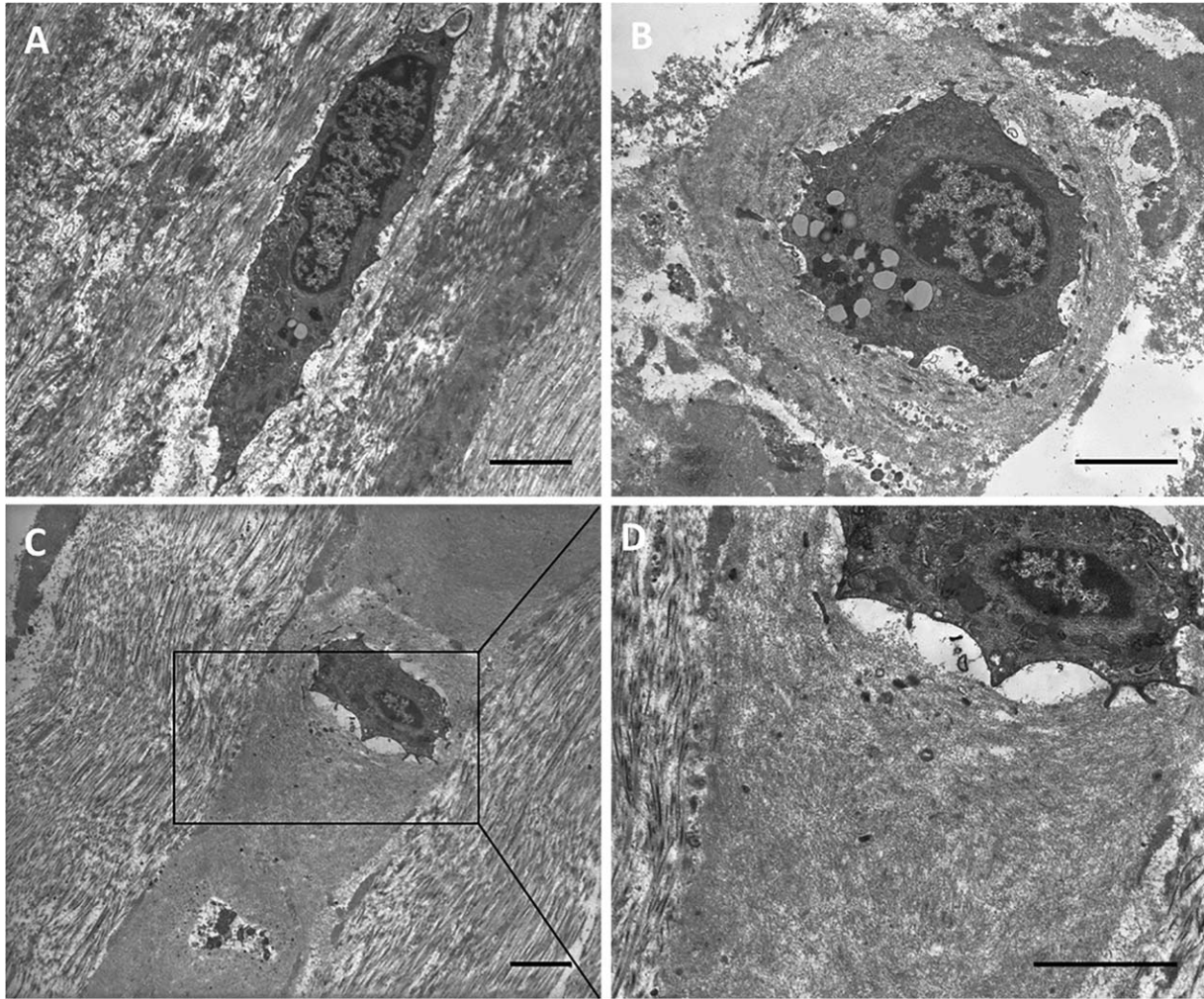


**Fig. 4.** TEM images of classical elongated fibroblasts (A) and prominent rounded cells (B, C, D) with the HA-rich matrix around them. Both cells are located in the loose connective tissue on the border with the fibrous layer. Scale bars: 3  $\mu\text{m}$ .

indicated by arrows in the Figure 1B. At greater enlargement they are clearly round, completely different from the classic elongated spindle-shaped fascial fibroblasts.

Human fascia lata stains prominently with Alcian Blue using 0.05 M  $\text{MgCl}_2$  (Fig. 1C,D), and by using the CEC principle we confirmed that the major GAG deposited in the ECM is HA (Scott and Dorling, 1965). When the  $\text{MgCl}_2$  concentration was increased to 2 M (Fig. 1E,F) there was a marked reduction in staining, and cells became clearer in the surrounding areas: the decreased staining associated with increased electrolyte concentration lends support to the concept that fascia is rich in HA and chondroitin sulfate (Schofield et al., 1975). Such staining is lost when the tissue sections undergo preliminary digestion with hyaluronidase (Fig. 1G,H). These cells do not have the typical elongated organization of fascial fibroblasts, but are more rounded, with cytoplasm restricted to the perinuclear region. Around them there is abundant ECM positive for all the HA-specific stains used in this work.

The HA nature of the ECM around these cells was confirmed using biotinylated HABP, which is highly specific for HA: Figure 2D,E shows the positive reaction in the cytoplasm and around some fibroblast-like cells. These areas became destained after digestion with hyaluronidase (Fig. 2F). Negative controls confirmed the specificity of the immunostaining (data not shown), whereas positive tissue controls evidenced positive reactions, especially around muscular cells of the tunica media of umbilical cord blood vessels (Fig. 2A,B), and negative reaction following digestion of the HA (Fig. 2C).

These positive-staining fibroblast-like cells were examined in semithin (Fig. 3) and ultrathin (Fig. 4) sections. Both images are distinguished from the loose connective tissue that separates from the fibrous fascial layer. These cells presented prominent nuclei, rounder in shape, and cytoplasm restricted to the perinuclear region with smaller and less elongated cellular processes than in fibroblasts. The matrix around them also appeared different from collagen fiber organization and

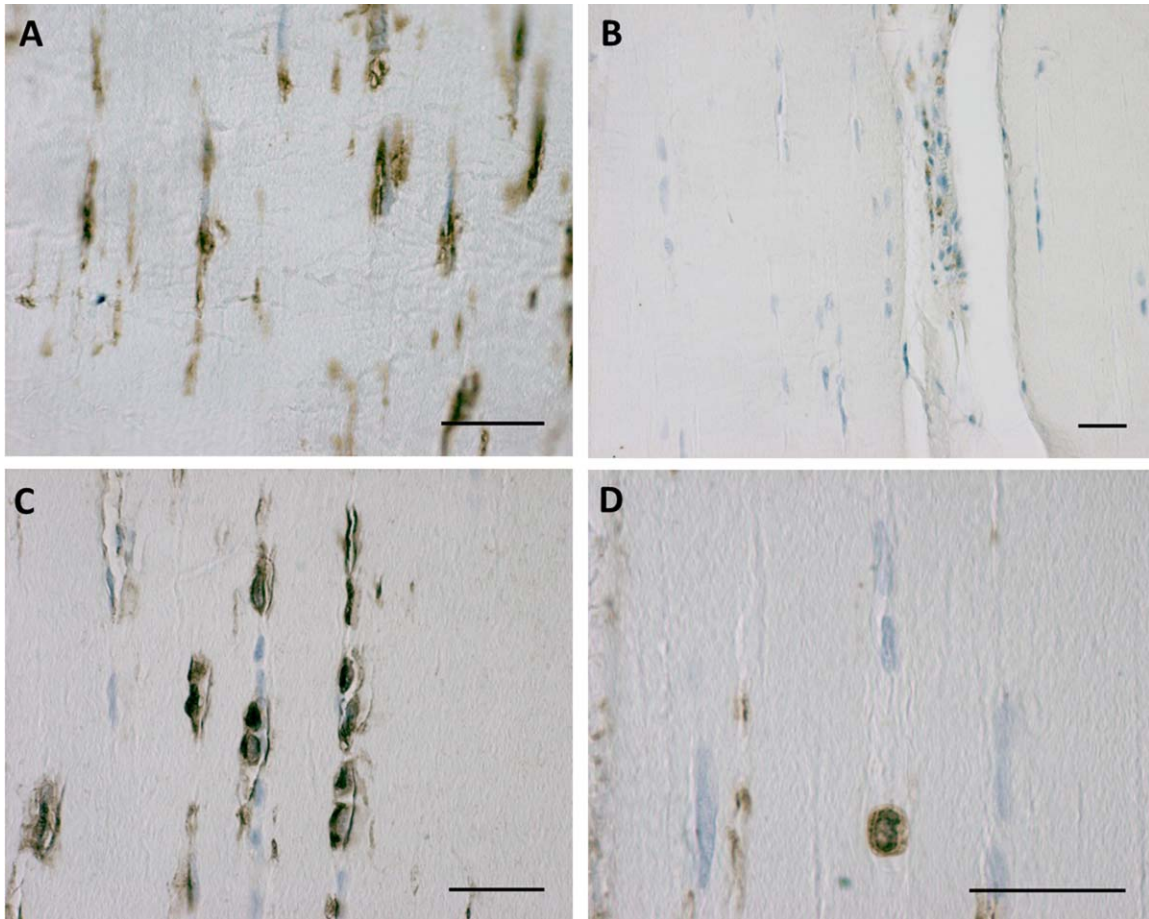


**Fig. 5.** Vimentin expression in human fascia lata (A), negative immunoreaction for CD68 (B), and S-100A4 positivity in fasciocytes (C,D). Scale bars: 50  $\mu$ m. [Color figure can be viewed at [wileyonlinelibrary.com](http://wileyonlinelibrary.com)]

the typical aspect of the glycosaminoglycans could be recognized (Fig. 4). This matrix corresponded to that stained with Alcian Blue. In all the samples of human fascia lata, the cells were located mostly at the

boundaries of the fibrous fascial sublayers, forming clusters of 3–4 cells. These clusters seem to demarcate the boundaries between the loose and fibrous connective tissue sublayers (Fig. 3A).

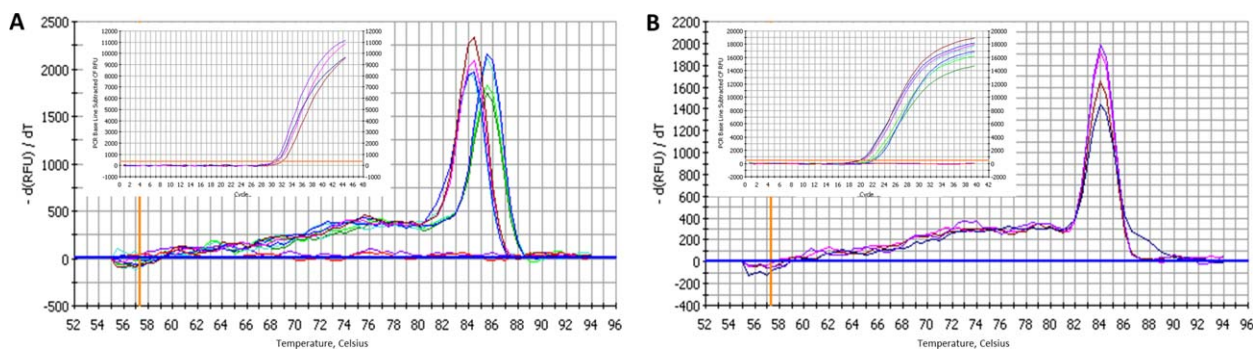


**Fig. 6.** Specific melting point plots of the PCR products using primers for RPS18 and RPLP0 (A), and for HAS2 (B) in human fascia lata. The baseline curves are the results using water, indicating the negative reactions. Insets show the real time PCR plots with cDNA, used to determine the Ct values. [Color figure can be viewed at [wileyonlinelibrary.com](http://wileyonlinelibrary.com)]

**TABLE 2. Comparison of Ct Values for Real Time PCR**

	$C_t$
RPS18	$20.7 \pm 1.1$
RPLP0	$21.9 \pm 0.15$
HAS2	$30.4 \pm 1.3$

The values are the means of at least three different experiments in triplicate.

Immunocharacterization of these cells demonstrated that they are modified fibroblasts, positive for the common intermediate filament fibroblast marker vimentin (Fig. 5A), but also positive for S-100A4, documenting a subclass of chondroid metaplasia (Masani et al., 1986; Klein et al., 1999) (Fig. 5C,D). The classical elongated fascial fibroblasts were not immunoreactive for S-100 (Fig. 5C,D). By manual counting,  $29.4 \pm 4.2\%$  of the total cells were immunopositive for S-100A4 and were therefore involved in chondroid metaplasia. Furthermore, immunohistochemical analysis with anti-CD68 proved that these fasciocytes were not derived from the monocyte/macrophage lineage (Bartok and Firestein, 2010). All the fascial cells were negative, except for the occasional macrophage and monocyte observed near vessels (Fig. 5B).

Finally, we studied the expression of HA synthase-2 by real time RT-PCR. We verified the specificity of the reactions and the absence of false amplicons; all samples had the same specific melting temperature for each amplified sequence, except for the water samples (the baseline curves) that indicate negative reactions (Fig. 6). The  $C_t$  values from PCR plots are reported in Table 2: the results confirmed the presence of HA synthase in fascial tissue, although with lower expression than the housekeeping genes RPS18 and RPLP0 (Ragni et al., 2013), as indicated by the higher  $C_t$  values: RPS18 had a mean  $C_t$  value of 20.7 (with more variability than the other housekeeping gene,  $\pm 1.1$  vs.  $\pm 0.15$ ); the mean  $C_t$  of RPLP0 was  $21.9 \pm 0.15$ ; the mean  $C_t$  for HAS2 was  $30.4 \pm 1.3$ . We used more than one verified reference gene to monitor any significant changes in  $C_t$  values continuously under our experimental conditions to avoid the reporting of uncorrected data (Svingen et al., 2015).

## DISCUSSION

In this work, we have characterized for the first time fibroblast-like cells in fasciae specialized for the biosynthesis of the HA-rich matrix. We have termed this new class of cells "fasciocytes." They are morphologically distinct from classical fibroblasts: the firsts have rounder nuclei, cytoplasm restricted to the perinuclear region, and smaller and less elongated cellular processes. Also, the location of these new cells is peculiar: the fibroblasts lie among the collagen fibrous bundles in the fibrous fascial sublayers, while the fasciocytes form small clusters along the surface of each fascial sublayer, defining the boundary between the fibrous sublayer and the loose connective tissue (Fig. 7). This peculiar location suggests that precise

regulation of the activity of these cells in HA production could modulate gliding between adjacent fibrous fascial sublayers, which seems to be strongly related to myofascial pain and range of movement (Langevin et al., 2011).

Our results clearly demonstrate that these fibroblast-like cells produce different elements of the ECM from classical fibroblasts. Fibroblasts produce collagen and elastic fibers; fasciocytes produce hyaluronan. Consequently, we can affirm that there are two different cell types in fasciae: one devoted to producing/regulating the fibrous component of the ECM, the other to producing/regulating the loose component. The fibrous component has a major role in transmitting force at a distance, while hyaluronan permits fascial gliding and autonomy among the various fibrous sublayers. It is evident that fasciae are appearing more and more complex, formed by various cells with different roles and probably responding to different inputs. The possibility of controlling/regulating the various cells precisely will probably make fascial alterations more responsive to more focused treatments and drugs. Indeed, it is already known that changes in HA concentration are associated with inflammatory and degenerative arthropathies (Temple-Wong et al., 2016) and that defects in fascial gliding can compromise the entire functionality of tissues and can generate pain (Bordoni and Zanier, 2014). Understanding what stimuli affect fascial cell activity will be fundamental to a better comprehension of the influence of the HA-rich matrix on tissue hydration and the lubrication of sliding surfaces (Stecco et al., 2011; Fakhari and Berklund, 2013), and to understanding the changes in the HA-rich matrix that occur in myofascial pain, as well as in other pathophysiologies affecting fascial tissue.

We demonstrated the expression of HA synthase in homogenates of fascial cells, and found that about 30% of fascial fibroblasts are fasciocytes. We think that the percentage of fasciocytes could vary depending on

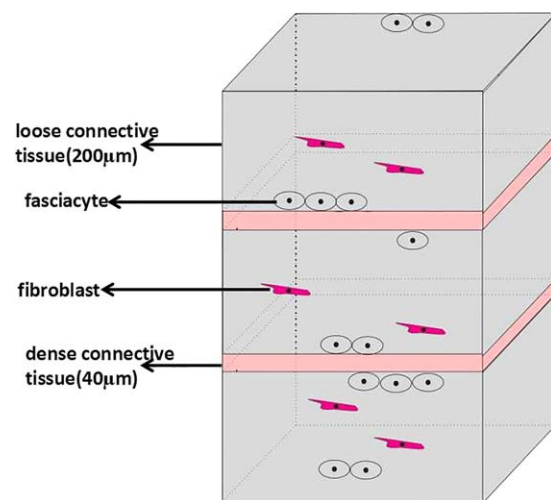


**Fig. 7.** Diagram of the layers of the deep fascia and the main location of the fasciocytes. [Color figure can be viewed at [wileyonlinelibrary.com](http://wileyonlinelibrary.com)]

**TABLE 3. Comparison Between the Main Features of Classical Fibroblasts and Fasciocytes**

	Fascial fibroblasts	Fasciocytes
Morphology	Elongated	Rounded shape
Location	Inside the loose connective tissue fascial layers	Especially between the fascial layers, at the borders
Alcian blue staining	Not all positive	More pronounced, inside the cells and around them
HABP	Not all positive	Positive
CD68	Negative	Negative
Vimentin	Positive	Positive
S100-A4	Negative	Positive
TEM	Extracellular matrix around cells has a collagen fibril architectures	Extracellular matrix around cells is enriched in proteoglycans

the stimuli that these cells undergo conducting them in the metaplastic phase.

Other tissues also contain fibroblast-like cells specialized for synthesizing and secreting high levels of HA. These include the synovial lining cells of joint capsules, where there are two distinct cell types: bone marrow-derived cells of the monocyte system (A cells) and specialized fibroblasts (B cells) (Iwanaga et al., 2000); and the hyalocytes in the eye (Sakamoto and Ishibashi, 2011), which express tissue macrophage marker (Holness and Simmons, 1993). The cells we have described in fasciae are negative for CD68, demonstrating that they are not of the monocyte/macrophage lineage. They are therefore likely to be related to chondrocytes, which are known to be S-100 protein-positive and specialized for HA synthesis.

In summary, the cells described seem to have specific morphology and location and a well defined function (Table 3). For these reasons we propose to call them "fasciocytes" as new class of fascia-associated cells.

## ACKNOWLEDGMENTS

We thank the Orthopedic Clinic of Padua for patient data and sample collection. The ultramicrotome was purchased through the funding for scientific equipment of the University of Padova (2013). Work by Caterina Fede was partially supported by a Fascial Manipulation Association grant.

## REFERENCES

Bartok B, Firestein GS. 2010. Fibroblast-like synoviocytes: Key effector cells in rheumatoid arthritis. *Immunol Rev* 233:233–255.

Benetazzo L, Bizzego A, De Caro R, Frigo G, Guidolin D, Stecco C. 2011. 3D reconstruction of the crural and thoracolumbar fasciae. *Surg Radiol Anat* 33:855–862.

Bhattacharya V, Chaudhuri GR, Mishra B, Kumar U. 2011. Demonstration of live lymphatic circulation in the deep fascia and its implication. *Eur J Plast Surg* 34:99–102.

Bordoni B, Zanier E. 2014. Clinical and symptomatological reflections: The fascial system. *J Multidiscip Healthc* 7:401–411.

Camenisch TD, Spicer AP, Brehm-Gibson T, Biesterfeldt J, Augustine ML, Calabro A, Jr, Kubalak S, Klewer SE, McDonald JA. 2000. Disruption of hyaluronan synthase-2 abrogates normal cardiac morphogenesis and hyaluronan-mediated transformation of epithelium to mesenchyme. *J Clin Invest* 106:349–360.

Castagna C, Viglietti-Panzica C, Panzica GC. 2003. Protein S100 immunoreactivity in glial cells and neurons of the Japanese quail brain. *J Chem Neuroanat* 25:195–212.

Chaitow L. 2014. Somatic dysfunction and fascia's gliding-potential. *J Bodyw Mov Ther* 18:1–3.

Chang SK, Gu Z, Brenner MB. 2010. Fibroblast-like synoviocytes in inflammatory arthritis pathology: The emerging role of cadherin-11. *Immunol Rev* 233:256–266.

Cowman MK, Schmidt TA, Raghavan P, Stecco A. 2015. Viscoelastic properties of hyaluronan in physiological conditions. *F1000Res* 4:622.

Fakhari A, Berkland C. 2013. Applications and emerging trends of hyaluronic acid in tissue engineering, as a dermal filler and in osteoarthritis treatment. *Acta Biomater* 9:7081–7092.

Fei F, Qu J, Zhang M, Li Y, Zhang S. 2017. S100A4 in cancer progression and metastasis: A systematic review. *Oncotarget* 8:73219–73239.

Fraser JR, Laurent TC, Laurent UB. 1997. Hyaluronan: Its nature, distribution, functions and turnover. *J Intern Med* 242:27–33.

Holness CL, Simmons DL. 1993. Molecular cloning of CD68, a human macrophage marker related to lysosomal glycoproteins. *Blood* 81:1607–1613.

Iwanaga T, Shikichi M, Kitamura H, Yanase H, Nozawa-Inoue K. 2000. Morphology and functional roles of synoviocytes in the joint. *Arch Histol Cytol* 63:17–31.

Jiang D, Liang J, Noble PW. 2007. Hyaluronan in tissue injury and repair. *Annu Rev Cell Dev Biol* 23:435–461.

Klein DM, Katzman BM, Mesa JA, Lipton JF, Caligiuri DA. 1999. Histology of the extensor retinaculum of the wrist and the ankle. *J Hand Surg Am* 24:799–802.

Kumka M, Bonar J. 2012. Fascia: A morphological description and classification system based on a literature review. *J Can Chiropr Assoc* 56:179–191.

Langevin HM, Fox JR, Koptiuch C, Badger GJ, Greenan-Naumann AC, Bouffard NA, Konofagou EE, Lee WN, Triano JJ, Henry SM. 2011. Reduced thoracolumbar fascia shear strain in human chronic low back pain. *BMC Musculoskelet Disord* 12:203.

Masani F, Iwanaga T, Shibata A, Fujita T. 1986. Immunohistochemical demonstration of S-100 protein in fibroblast-like cells of the guinea-pig heart. *Arch Histol Jpn* 49:117–127.

McCombe D, Brown T, Slavin J, Morrison WA. 2001. The histochemical structure of the deep fascia and its structural response to surgery. *J Hand Surg Br* 26:89–97.

Mohr W, Kuhn C, Pelster B, Wessinghage D. 1985. S-100 protein in normal, osteoarthrotic, and arthritic cartilage. *Rheumatol Int* 5:273–277.

Ragni E, Viganò M, Rebulli P, Giordano R, Lazzari L. 2013. What is beyond a qRT-PCR study on mesenchymal stem cell differentiation properties: How to choose the most reliable housekeeping genes. *J Cell Mol Med* 17:168–180.

Sakamoto T, Ishibashi T. 2011. Hyalocytes: Essential cells of the vitreous cavity in vitreoretinal pathophysiology?. *Retina* 31:222–228.

Schofield BH, Williams BR, Doty SB. 1975. Alcian Blue staining of cartilage for electron microscopy. Application of the critical electrolyte concentration principle. *Histochem J* 7:139–149.

Scott JE, Dorling J. 1965. Differential staining of acid glycosaminoglycans (mucopolysaccharides) by alcian blue in salt solutions. *Histochemistry* 5:221–233.

Seccia TM, Carocchia B, Gioco F, Piazza M, Buccella V, Guidolin D, Guerzoni E, Montini B, Petrelli L, Pagnin E, Ravarotto V, Belloni AS, Calò LA, Rossi GP. 2016. Endothelin-1 drives epithelial-mesenchymal transition in hypertensive nephroangiosclerosis. *J Am Heart Assoc* 5:e003888.

Sedaghat F, Notopoulos A. 2008. S100 protein family and its application in clinical practice. *Hippokratia* 12:198–204.

Stecco A, Meneghini A, Stern R, Stecco C, Imamura M. 2014. Ultrasonography in myofascial neck pain: Randomized clinical trial for diagnosis and follow-up. *Surg Radiol Anat* 36:243–253.

- Stecco C, Gagey O, Belloni A, Pozzuoli A, Porzionato A, Macchi V, Aldegheri R, De Caro R, Delmas V. 2007. Anatomy of the deep fascia of the upper limb. Second part: Study of innervation. *Morphologie* 91:38–43.
- Stecco C, Stern R, Porzionato A, Macchi V, Masiero S, Stecco A, De Caro R. 2011. Hyaluronan within fascia in the etiology of myofascial pain. *Surg Radiol Anat* 33:891–896.
- Svingen T, Letting H, Hadrup N, Hass U, Vinggaard AM. 2015. Selection of reference genes for quantitative RT-PCR (RT-qPCR) analysis of rat tissues under physiological and toxicological conditions. *PeerJ* 3:e855.
- Taşdemir A, Oğuz A, Ünal D, Tuna Ö. 2014. Metaplastic carcinoma of the breast: A rare carcinoma with chondroid metaplasia. *Ulus Cerrahi Derg* 30:57–59.
- Temple-Wong MM, Ren S, Quach P, Hansen BC, Chen AC, Hasegawa A, D’Lima DD, Koziol J, Masuda K, Lotz MK, Sah RL. 2016. Hyaluronan concentration and size distribution in human knee synovial fluid: Variations with age and cartilage degeneration. *Arthritis Res Ther* 18:18.
- Yammani RR, Long D, Loeser RF. 2009. Interleukin-7 stimulates secretion of S100A4 by activating the JAK-STAT signaling pathway in human articular chondrocytes. *Arthritis Rheum* 60:792–800.